

Nondestructive evaluation of sintering and degradation for rotational molded polyethylene
F.P.C. Gomes, M.R. Thompson*

*Department of Chemical Engineering, CAPPA-D/MMRI
McMaster University, Hamilton, Ontario, Canada*

Submitted to: POLYMER DEGRADATION AND STABILITY

March 2018

* Author to whom correspondence should be addressed.

Tel: (905) 525-9140 x 23213

Fax: (905) 521-1350

mthomps@mcmaster.ca

Nondestructive evaluation of sintering and degradation for rotational molded polyethylene

ABSTRACT

Developments in new sensor technologies and data processing are helping to increase the number of applications of nondestructive characterization methods. In this study, two major physiochemical phenomena affecting product quality of rotationally molded polyethylene parts, namely sintering and degradation, were evaluated using both traditional characterization techniques and a newer alternative ultrasonic-based method. Oven temperature and heating cycle time were controlled to produce six different process conditions for rotomolding. Increasing peak internal air temperature (PIAT) inside the mold produced a reduction in surface voids (pitting) and increased the impact strength for produced parts, which can be related to greater densification during sintering. Contrary to these characterizations denoting improved part quality, degradation was detected for PIAT above 220 °C by an increase in surface carbonyl groups by Fourier-transform infrared spectroscopy (FT-IR) and an increase in zero-shear viscosity, both relatable to thermo-oxidative free radical reactions. The newly proposed monitoring technique applying propagating ultrasonic guided waves showed that its data-rich spectral features based on harmonic frequencies were positively correlated to the same sintering and degradation properties observed above. Coupled with multivariate statistical analysis, the nondestructive ultrasonic technique shows great promise for combining multiple analyses in a single sensor technology, making it well suited to the implementation of advanced manufacturing methodologies in polymer processing practices.

Key-words: nondestructive evaluation, ultrasonic, impact, degradation, polyethylene

1. Introduction

Industry has been changing in recent years with the introduction of digital informatics and the growing efforts towards advanced manufacturing. The focus in manufacturing is moving towards the development of tools that will allow more reliability, flexibility and capacity for optimizing processes. These tools are not simply hardware but rather process information collection with improved data processing, new control strategies and faster communications [1]. Examples of these advancements in polymer processing have been gradually presented [2–5]. Those studies have shown how sensor signals conveying single variable descriptive data can improve a process; however, the challenge becomes how to incorporate more complex data-heavy techniques and sensors that can expand the possibility of the envisaged framework for advance manufacturing in polymer processes.

The production of hollow parts using rotational molding involves the melting then densification of polymer powders without the aid of external compression or shear forces; these steps referred to as sintering and are similarly seen in the newer 3-D printing technology known as selective laser sintering (SLS) [6]. This method is widely used for production of large shapes such as storage tanks, marine shells and other diverse components. Final quality of rotational molded parts is highly dependent on the extent of two contrasting phenomena: sintering and thermo-oxidative degradation [7]. During the melting stage of the process, liquid bridges form among the particles trapping air bubbles that need to vanish during the subsequent densification stage, all occurring under moderate temperatures above the polymer melting point for a moderate period of time [8]. If these bubbles are not removed, the produced parts will have poor mechanical properties [9]. Due to the nature of the hollow mold, the polymer melt will be constantly exposed to oxygen and maintained at high temperatures, which will promote thermo-oxidative degradation and also alter mechanical properties [10]. Polyethylene degradation leads to discoloration, poor long term mechanical properties and possibly embrittlement due to chain crosslinking [11]. Process reliability depends on monitoring features of the produced part related with these two processes, and thus the selection of characterization methods plays a key role in

ensuring production quality.

Currently, the manufacturing industry relies on destructive tests to assess the quality of these parts. Impact strength is the most heavily relied upon property for rotational molding, being easily affected by process conditions and readily highlighting issues related to incomplete sintering [7,12]. Other similar options are to evaluate elastic modulus, hardness [13] and fracture toughness [14]. Chain branching and cross-linking during thermo-oxidative degradation will increase the viscosity of polyethylenes typically used in rotational molding, which can be seen by measurements like melt flow index [15] or parallel plate rheometry [16]. However, none of these tests are applicable to quality assurance of each part produced, instead requiring a small number of parts from each production run to be diverted for testing and where those tests can take hours before the processor is informed whether the process conditions were acceptable. Therefore, in order to adopt practices of increased process reliability and flexibility, applications of nondestructive techniques are desirable.

Spectroscopic methods are examples of nondestructive techniques that have seen limited use in manufacturing, mostly because of the large amounts of data collected and expertise required by the user for their interpretation, but there have been rare examples of their use for rotational molding albeit not for quality assurance. Fourier-transform infrared spectroscopy (FT-IR) was used to identify oxidation products at the surface of rotomolded parts [17]. Additionally, X-ray diffraction was used to evaluate changes in crystal morphology for evidence of degradation [18]. Neither technique is readily integrated into a manufacturing process and these instruments are expensive. On the other hand, no reports have been made of ultrasonic testing in rotational molding, even though it has been shown as a powerful technique to evaluate the structure of materials for other processes. Traditional single variable ultrasonic methods are very efficient for density measurement by relating this property to changes in velocity or attenuation of a sound wave propagating through a sample, with noted examples for different polyolefins [19,20] and polymer foams [21]. However, recent developments in the field of ultrasonics have turned the focus towards the generated spectrum from a propagated signal as means to

interpret structural features of polyethylene samples [22]. Specifically, a new approach analyzing the amplitude of spectral harmonics has been successfully applied to evaluate changes in crystal morphology using ultrasonic guided waves [23]. This advancement in ultrasonic methods relies upon small out-of-plane mechanical strain to correlate structural features of a material to resonant frequencies in the collected signal; the method did not permanently damage a part but not all shapes molded can be easily distorted and hence a better training method is needed to extract the information from these complex signals and correlate with quality properties. The challenge of any new spectroscopic techniques, however, is how to correlate the large quantity of spectral data with one or multiple quality properties currently of interest to the industry, and consequently their incorporation in the production line for improved process operations.

This study compares the effectiveness of a ultrasonic nondestructive spectroscopic technique to replace multiple traditional destructive and nondestructive tests needed to evaluate both sintering and degradation processes for rotational molded polyethylene samples. An important goal of the work was to better highlight the benefits of ultrasonic spectroscopic techniques in polymer processing.

2. Methods

2.1. Material

For this study, a high density polyethylene (ExxonMobil™ HD 8660.29) powder of 35 Mesh size was provided by Imperial Oil Ltd. The resin has a melt index of $I_2 = 2$ g/10 min (ASTM D1238) and stated crystal melting temperature of 129 °C, according to the vendor.

2.2. Rotational molding

Samples were prepared using a laboratory-scale uniaxial rotational molding device coupled with a data acquisition system for monitoring of the internal mold air temperature as well as controlling the oven temperature. A shot of 100g was loaded to the mold. The oven was pre-heated to the designated temperature and the batch run was started when the mold was moved inside. Each batch run followed a specific heating cycle time, and after a designated period of time the mold was removed

from the oven to be cooled by forced air applied at approximately 2.5 m/s (measured by a digital anemometer). The mold was cooled to 80 °C before removal of the sample. The final samples resembled a cube missing its front and back panels, with each molded wall panel being approximately 85 mm x 85 mm by 3 mm thick cut from the sample using a band saw. Each chosen heating cycle condition was used to prepare at least three replicate samples.

2.3. Surface analysis

A square area of 40 mm x 40 mm was isolated on the outer facing surface of a wall panel (mold-side facing) using adhesive tape. A low viscosity lubricant containing a mixture of micron-sized copper and graphite particles (Permatex) was brushed over the designated area, with the excess wiped away. By this procedure, surface holes were filled with the dark colored lubricant so they would be more clearly seen. Images were taken with a digital camera and processed with image analysis software to estimate the surface area coverage of voids per sample.

2.4. Fourier-transform infrared spectroscopy

Infrared vibrational spectroscopy (FT-IR) was performed with a Thermo Scientific Nicolet 6700 in attenuated total reflection (ATR) mode. Both internal and external surfaces of the panels were analyzed by FT-IR. Mid-range wavenumbers between 700 to 4000 cm^{-1} were scanned at a resolution of 0.4 cm^{-1} and an average of 32 scans was reported. After baseline correction, peaks were identified using a Voigt window search and normalized based on the reference peak at 2915 cm^{-1} .

2.5. Ultrasonic spectroscopy

Panel wall specimens were tested using an ultrasonic guided waves test apparatus, as previously reported [23]. The distance between ultrasonic transducers was kept at 55 mm. Each resultant spectrum per specimen was produced from the combined averaging of 31 different signals corresponding to a stepwise frequency sweep from 135 to 165 kHz, incremented by steps of 1 kHz. Three panels were tested per sample.

2.6. Impact test

After samples were tested using the non-destructive methods of FT-IR and ultrasonic, each wall panel was characterized for impact behavior using a dart impact test. Samples were grouped based on the processing conditions, thus totalizing 12 tests per group. Test samples were pre-conditioned in a freezer at -40 °C for 24 h. For each group, an initial height was selected and moved using the staircase method based on the resultant failure or non-failure. A standard 6.804 kg dart was used with varying height steps of 0.1524 m (0.5 ft). A resultant average failure height was converted to impact energy in joules (J) and reported for each group.

2.7. Rheology

Specimens from the molded samples were evaluated for their viscosity with a Discovery HR-2 TA Instruments configured to operate with 25 mm parallel plates. A small square was cut from the wall panel of a sample and melted in the plates at 190 °C. After melting, the excess polymer was removed and the gap between plates was reduced to 1.5 mm. A frequency sweep spanning 0.1 to 200 s⁻¹ was performed at a strain of 0.15. Zero-shear viscosity was estimated using the Cross model.

2.8. Multivariate statistical analysis

Spectral data collected from the ultrasonic tests was used to construct a statistical model to differentiate molded samples in relation to both sintering and degradation processes. Two projections to latent structures (PLS) models were built using measurements from traditional tests as training references. The statistical software R was used with the library 'pls'. Ultrasonic spectra matrix data was pre-processed with a baseline correction for the sintering model and additional normalization for the degradation model. The number of components chosen were based on the minimum root-mean square of prediction error (RMSEP) for an internal cross-validation using the leave-one-out method.

3. Results and Discussion

3.1. Process exploration

Two factors were considered for the experimental design: oven temperature, that influenced the heating rate; and batch time, considered to be the duration that the mold stayed inside the oven. It was

expected that both would influence the profile of the mold temperature, having longer batch time and higher heating rates having a positive correlation with the maximum temperature reached. A two level factorial with center point was designed, with lower and upper limits of 300 and 340 °C for the oven temperature, and 12 minutes and 18 minutes for batch time. A sixth point was added to further explore the upper limits of heating rate at the center point batch time of 15 minutes. Experiments were monitored using a thermocouple installed in the rotational arm that measured the internal mold air temperature. Resulting internal temperature profiles, shown in Figure 1, demonstrate the positive effect of the two factors towards reaching the highest possible maximum temperature inside the mold. A common way of interpreting variations between rotational molding batches is to refer to the maximum temperature inside the mold as the peak internal air temperature (PIAT). Although this measurement does not reflect the complete history of the heating and cooling cycle, it can be used as a single variable descriptor for the effectiveness of sintering. Thus, for the next sections, experimental results will be referenced based on their values of PIAT.

From the results presented in Table 1 it was observed that operating at the lower factor levels, samples produced lower impact strength and higher surface voids in the molded parts, due to incomplete sintering. Conversely, for the higher factor levels, a significant increase in zero-shear viscosity was observed, indicating crosslinking due to thermo-oxidative degradation. Longer heating cycles at a low heating rate produced a slight improvement in impact strength compared to shorter heating cycles at higher heating rates, even though both approaches reached similar PIAT.

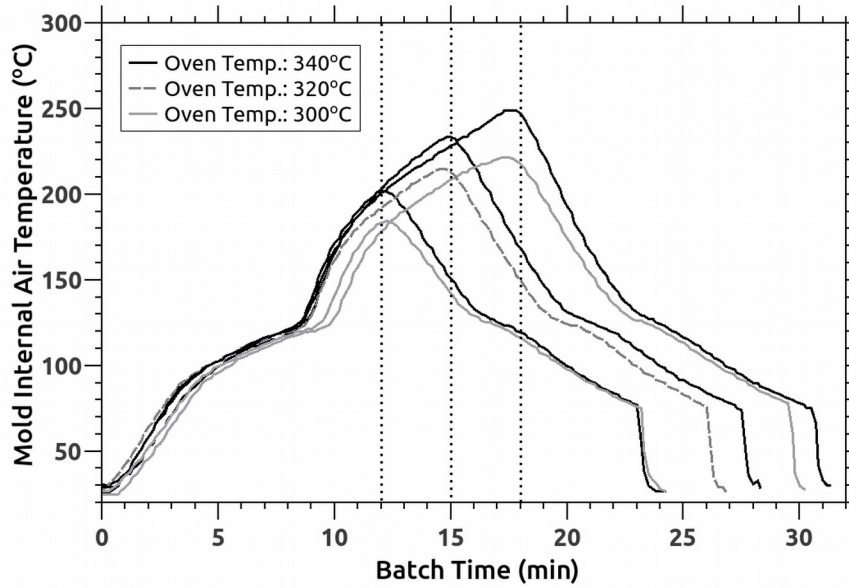


Fig. 1 – Rotational molding temperature profiles (vertical dashed lines indicate the removal of the mold from the oven and the end of the heating cycle)

Table 1 – Results from experimental design

Process conditions		Product characterization			
Oven Temperature – °C	Heating time - min	Peak internal air temperature PIAT) – °C	Impact Energy – J	Surface voids area coverage – %	Zero-shear viscosity – Pa-s
300 (-1)	12 (-1)	181 ± 5	0.31	6.6 ± 1.1	6,403 ± 212
340 (+1)	12 (-1)	200 ± 2	0.37	4.5 ± 0.9	6,496 ± 44
300 (-1)	18 (+1)	218 ± 5	0.50	1.8 ± 0.8	7,242 ± 741
340 (+1)	18 (+1)	250 ± 3	0.65	0.4 ± 0.2	12,689 ± 714
320 (0)	15 (0)	215 ± 6	0.43	3.6 ± 1.9	6,868 ± 893
340 (+1)	15 (0)	238 ± 4	0.65	0.6 ± 0.2	12,033 ± 84

3.2. Sintering

Based on changes in the temperature profiles shown in Figure 1, the powder cohesion and

melting phase took between 8 minutes to 10 minutes. After this point, the additional heat energy was directed to the densification or melt coalescence process by removal of the air bubbles formed during initial melting. Observations from the surface of the samples provided a direct estimation of the residual concentration of bubbles at the end of a batch trial. Figure 2 presents a comparison of images and calculated coverage area of surface voids (i.e. pitting) from the samples with different PIAT and a control sample (compression molded for 10 minutes at 175 °C and 2 kPa, then quenched using water-cooled plates); surface coverage area is being considered as a two dimensional representation of the void content or porosity of the overall sample in this work. A high PIAT produces molded parts with lower value of residual bubbles. A maximum of 5% to 7% was observed for the surface coverage area with low PIAT whereas near-negligible values below 1% (still higher than the control) were reported for samples with PIAT above 230 °C. From Figure 2c is possible to visually observe large residual bubbles at the end of the sintering process, those will take a longer time to disappear even at high mold temperatures, as the removal rate of bubbles will be proportional to the porosity of the part (which is related to bubble size and the number of bubbles present) [24].

The extent of bubble removal is directly yet inversely related to impact properties. As shown in Figure 3, samples with higher coverage area of surface voids showed a lower value of impact energy. Those samples at the low end of the range of impact properties often demonstrated a brittle failure during testing with easy crack propagation found between voids. A progressive increase in impact strength was observed with reducing porosity, which correspondingly denoted a transition between brittle to ductile failure with increased fibrillation observed at the point of impact. No significant increase in impact energy was observed for samples above 230 °C, which corresponded to the lower observed range for the surface voids coverage area. The maximum impact values observed were lower than obtained by the control samples, prepared by compression molding.

The multiple methods of analysis mentioned above are standards for the industry to provide a good estimation for the degree of sintering, but do not reflect the overall concentration of voids

internally and at least in the case of the surface analysis, might not be practical for all mold profiles or different types of product finishes. An alternative yet still traditional nondestructive test method for porosity is to use ultrasonics to infer density based on the propagation of sound waves through the part; while this approach is not what is ultimately to be disclosed in this paper regarding the perceived strength of ultrasonic analysis, it provides a context to build towards that discussion. Using the same propagation distance for samples of similar dimensions, variations in the maximum signal amplitude of a propagating sound waves (on a time domain) can be directly connected with the attenuation caused by the presence of bubbles in the part. Figure 4 shows the increased ultrasound amplitude found with increasing PIAT, thus presenting a good correlation with the impact energy of this group of samples. Samples with PIAT above 230 °C showed amplitude values comparable to the control sample. A lower limit for the application of this method is the detection of signals for samples with high value of attenuation.

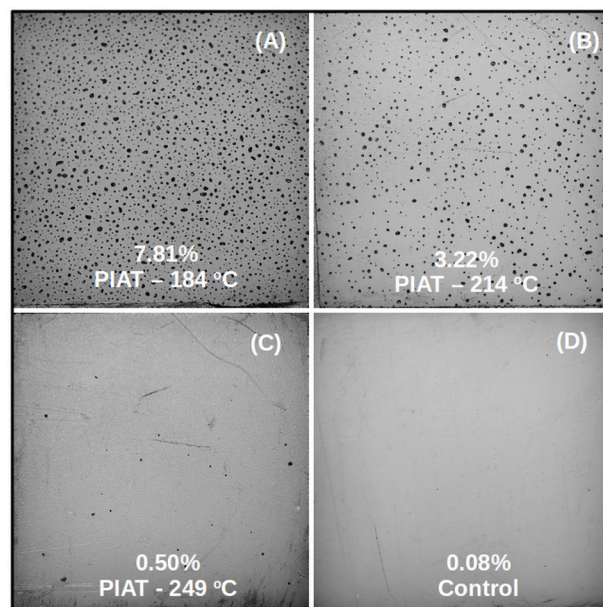


Fig. 2 – Surface image analysis for voids area coverage with increasing PIAT (percentage indicates voids area related to the total area)

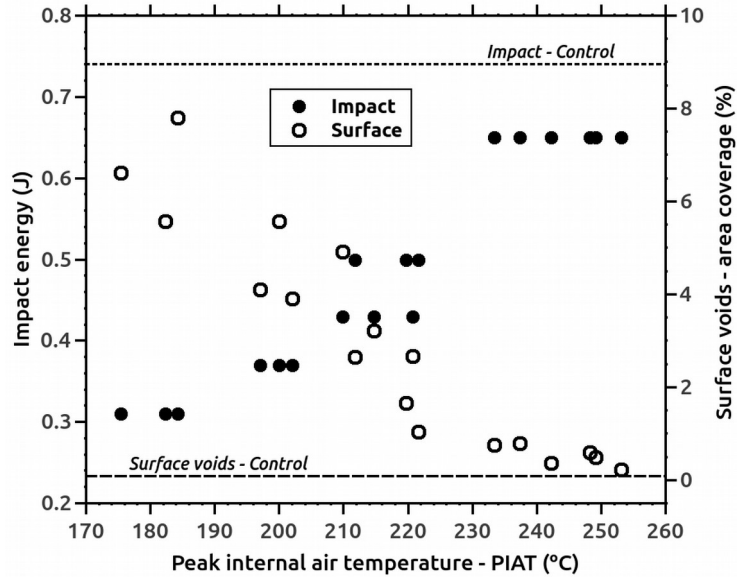


Fig. 3 – Surface voids area coverage and impact energy for rotational molded samples with different peak internal air temperatures (horizontal dashed lines indicate reference values for the control samples)

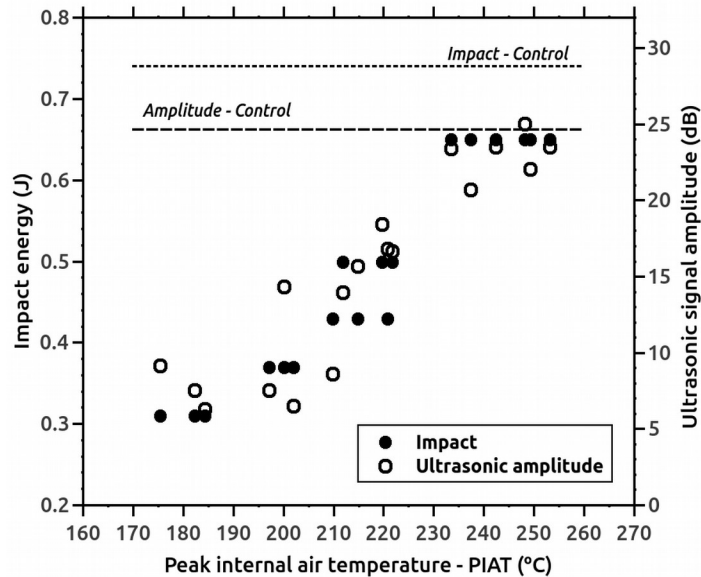


Fig. 4 – Ultrasonic signal amplitude and impact energy for rotational molded samples with different peak internal air temperatures (horizontal dashed lines indicate reference values for the control samples)

3.3. Degradation

Effects of degradation were investigated using FT-IR spectroscopy to monitor for oxidation products at the surface of the molded samples. Both surfaces of panel cut from a sample were tested ; however, only the internal surfaces showed any development of carbonyl compounds which were detected at 1715 cm^{-1} ; thermo-oxidative degradation is expected to be predominantly on inner surfaces of a part due to their continuous exposure to trapped air at high temperatures during rotational molding, while outer layers are effectively shielded since the antioxidants present would not be fully consumed prior to their isolation from the internal air [7]. Figure 5 gives FT-IR spectra showing the appearance of the oxidation product for inner surfaces of samples with PIAT above $230\text{ }^{\circ}\text{C}$. For samples molded with PIAT lower than this threshold it can be expected that antioxidants were not depleted.

Alternatively, rheology can be used as an indirect method to evaluate degradation. During thermo-oxidative degradation, free radicals are formed increasing the chances of chain cross-linking for polyethylene. This will have a significant effect on the molecular weight distribution, thus affecting the viscosity [16]. A marked increase in degradation is seen by the significant rise in zero-shear viscosity for samples with PIAT higher than $220\text{ }^{\circ}\text{C}$, observable in Figure 6. Comparing the trends between the rheological and infrared analysis, the viscosity measurements seemed to provide better sensitivity to degradative changes, because of its bulk nature of assessment rather than being limited to only the top several microns of polymer species near the surface of the panel by FT-IR. Although, other references have mentioned an effect of crosslinking on impact strength, which could be initially beneficial but ultimately reduce the quality at very high PIAT values (above $250\text{ }^{\circ}\text{C}$) [11], none of the mechanical detrimental effects were observed for the process conditions investigated in this study.

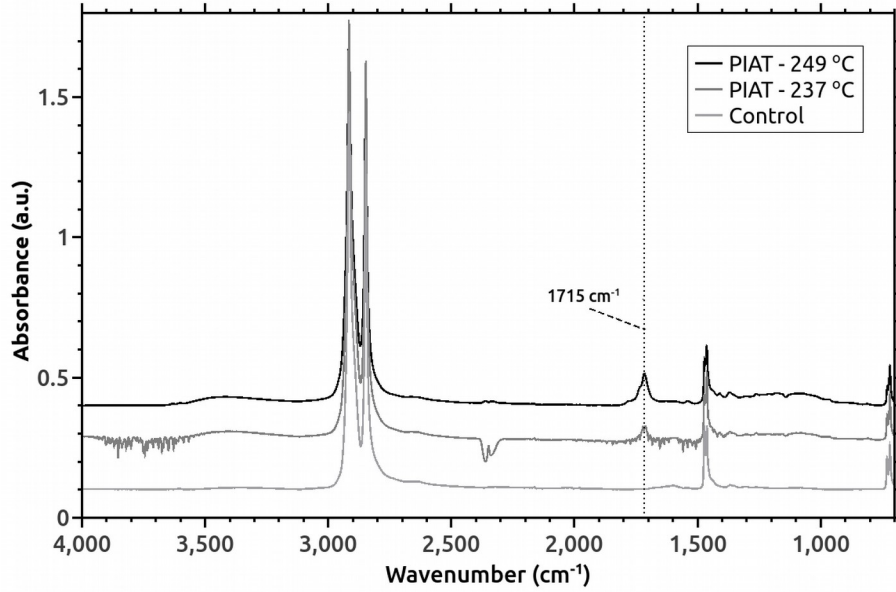


Fig. 5 – FT-IR spectra from the internal surface of samples with different PIAT highlighting the appearance of subproducts of thermo-oxidative degradation (vertical dashed line indicates the wavenumber of the carbonyl peak)

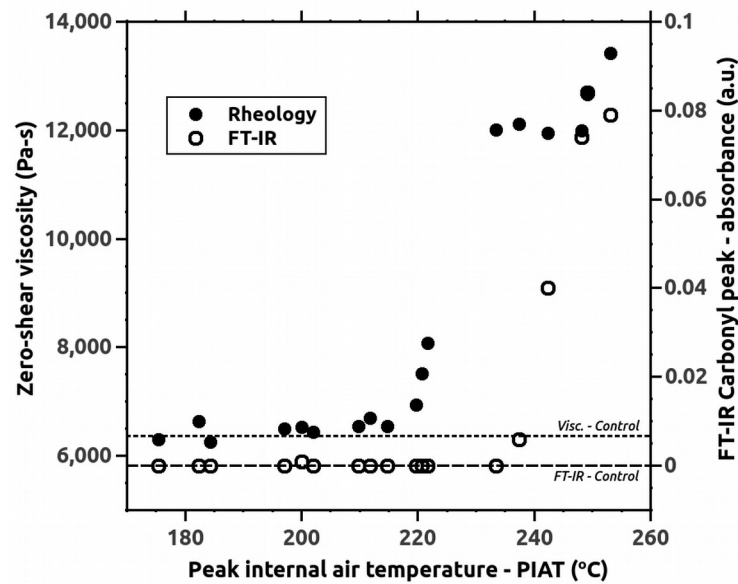


Fig. 6 – Zero-shear viscosity and absorbance level of carbonyl peak from FT-IR for samples with different PIAT (horizontal dashed lines indicate reference values for control sample)

3.4. Ultrasonic spectrum with multivariate statistical analysis

Results from the methods previously described in this study presented good but limited response to either sintering or degradation quality related features. With the objective to evaluate the quality of samples related to both phenomena simultaneously, a new approach was tested using spectroscopic analysis of the ultrasonic wave propagation. Figures 7 and 8 show examples of ultrasonic spectra from parts with increasing PIAT. For the first case, looking at samples selected for showing little or no level of degradation, an increase was observed in Figure 7 for the peak corresponding to the frequency range of the excitation signal (between 135-165 kHz) reflecting a decrease in attenuation of the propagated wave due to fewer voids for a higher PIAT. This behavior is similar to what was found from the time domain analysis, as demonstrated in Figure 4, but now identified as being localized to specific resonant frequencies. In Figure 8, a second group of samples was selected with similar extent of sintering but differing degrees of thermo-oxidative degradation. The resultant spectra were normalized before plotting and show an increase in the third harmonic range (frequencies from 405-495kHz) related to the excitation frequencies with increasing PIAT. This variation in the ratio between the peak amplitude of higher harmonics was highlighted in a previous publication being a descriptor of morphological changes within semi-crystalline structures after applied plastic deformation or solvent absorption [23]. Although, so far, results presented in this section have demonstrated that features of the ultrasonic spectrum can be correlated with sintering and degradation phenomena, interpretation of this spectroscopic data for different molded parts is not trivial and cannot be compared to the descriptors used in previous study that observed the progression of modifications for the same sample. In order to make definitive correlations based on the variance contained in the ultrasonic spectral dataset of several molded parts with traditional characterization methods, an inferential model using latent variables statistical methods was developed.

Two PLS models were constructed using the full spectral dataset from the ultrasonic measurements of the molded samples. Table 2 presents a summary of conditions used as some general descriptors to develop these models. Data from the coverage area of surface voids was used as

reference information for calibrating the sintering model, while results from zero-shear viscosity were applied for the degradation estimation. An internal cross-validation, based on the leave-one-out method, estimated a root-mean squared error of prediction (RMSEP) for several number of components. The ultimate number of four components was chosen to fit the model based on the case with lower value of error, 1.37% for the sintering model and 2524 Pa-s for the degradation model. This procedure helped to avoid over fitting but still be able to explain the correlation between the matrices introduced for calibration. The value of RMSEP showed in Table 2 demonstrates the error for the model to predict an internal value. Moderate values of explained variance were observed for both models, which shows how much of the variance from the original data was used in the correlation between the training variable and the calibration matrix.

Figures 9 and 10 present the model predictions superimposed with the observed values. Errors in prediction were higher for the sintering model at high concentration of voids (values of coverage area of surface voids higher than 5%), mostly due to limitations imposed on the method by the high attenuation of the propagated signal. A classification of the inferred properties was proposed by comparing the estimated value with two control groups, formed by samples selected from the training group that had complete sintering (coverage area of surface voids <1.0%) and no degradation (zero-shear viscosity <7000 Pa-s), with six and nine samples per group, respectively. The model predictions were statistically compared with the reference groups and if the value exceeded a 98% confidence interval threshold, they would be classified as incomplete sintering or degraded samples. This classification criteria represents the capacity of the model constructed with the ultrasonic spectroscopic data to distinguish a sample with unsatisfactory properties. Results of this classification are shown in Figures 9 and 10 highlighted as solid or hollow circles, and a group separation is observed around a PIAT of 220 °C, marking the point of end of the sintering process and acceleration of degradation process.

A group of four samples was randomly chosen from the original batch runs and was not

introduced in the model during its training to serve as a validation group. Table 3 shows both the prediction values and the classification of these samples for sintering and degradation. These results support our assertion that the model is capable of predicting major changes for both phenomena correctly, recognizing for increasing PIAT values that the prediction should be for coverage area of surface voids to decrease while zero-shear viscosity increases accordingly.

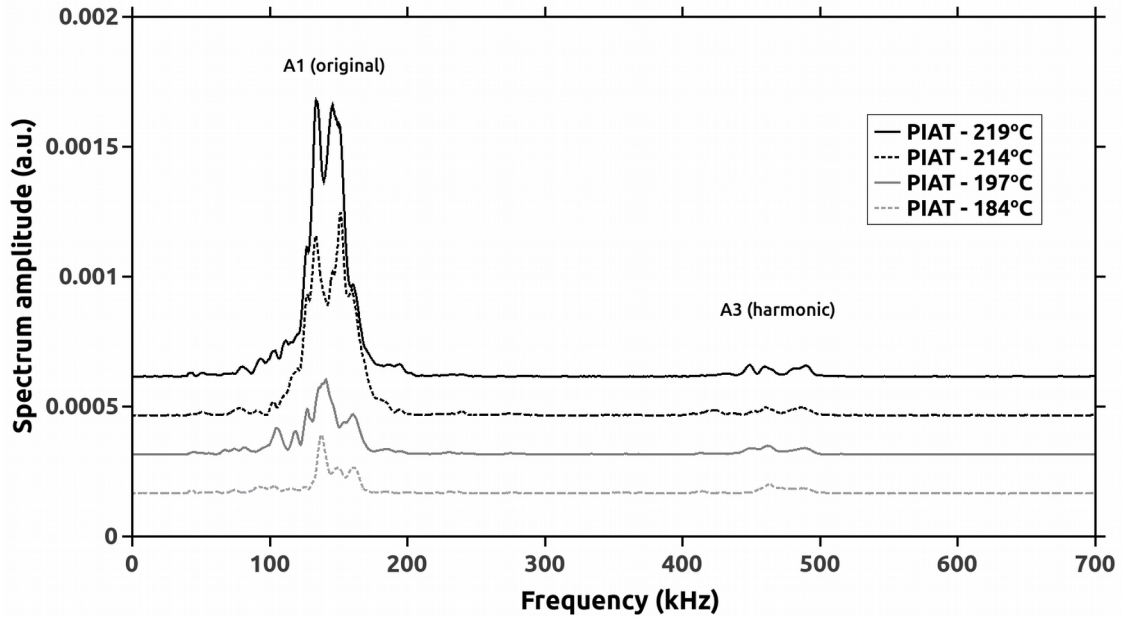


Fig. 7 – Ultrasonic spectra for samples with different PIAT presenting different levels of sintering (A1 indicates the peaks at original excited frequencies and A3 indicates the peaks at third harmonic range)

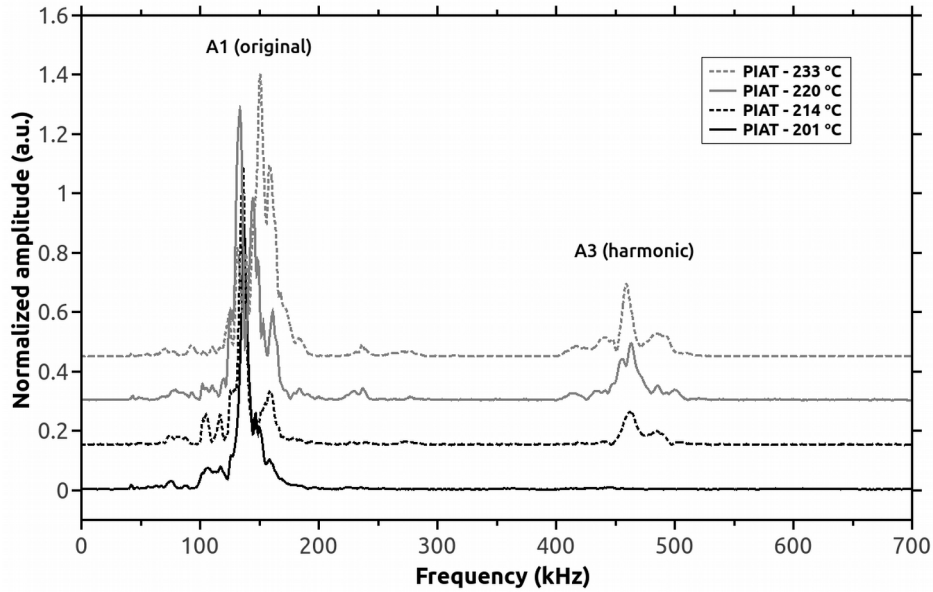


Fig. 8 – Ultrasonic spectra for samples with different PIAT presenting different levels of degradation (A1 indicates the peaks at original excited frequencies and A3 indicates the peaks at third harmonic range)

Table 2 – Summary of PLS models

Number of experimental samples for training	15	
Number of ultrasonic spectra per sample	3	
Points per spectra (frequencies)	2,500	
Total number of points for data matrix	112,500	
Model	Sintering	Degradation
Variable used for training	Surface voids area coverage	Zero-shear viscosity
PLS - Number of components	4	4
Internal cross-validation error-RMSEP	1.37%	2524 Pa-s
Variance explained of the training variable	80.9%	73.0%
Variance explained of the data matrix	83.5%	58.6%

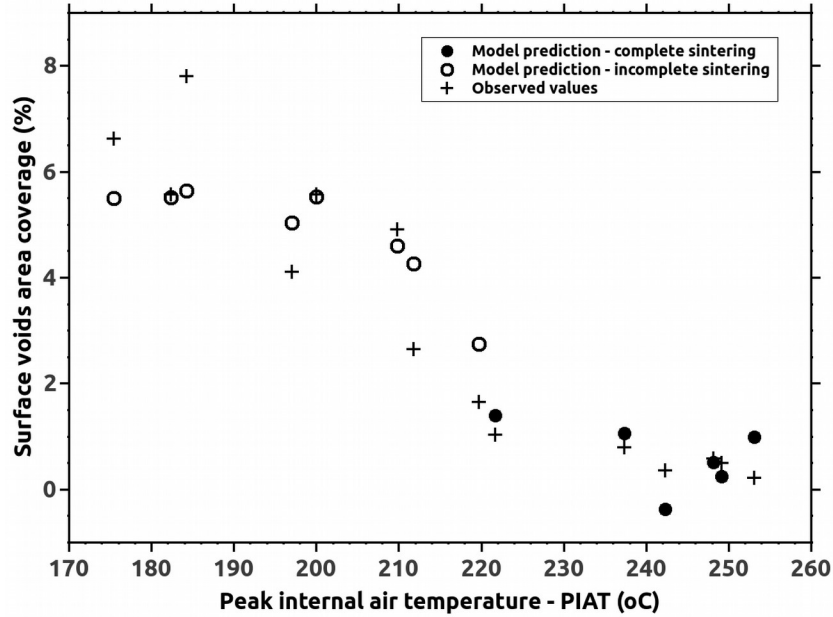


Fig. 9 – Prediction results for surface voids area coverage of samples with different PIAT using a PLS model (classification of incomplete sintering based on statistical comparison with reference group, for a p-value<0.02)

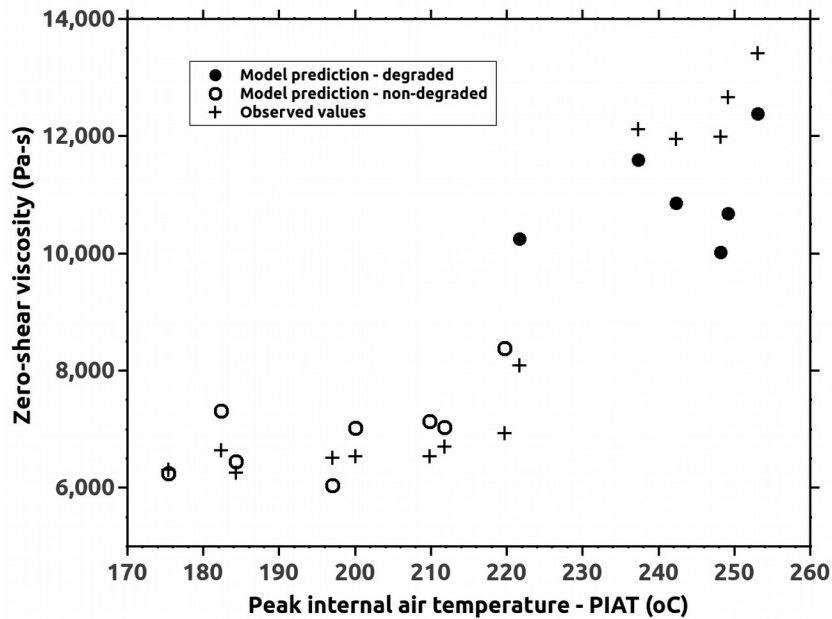


Fig. 10 – Prediction results for zero-shear viscosity of samples with different PIAT using a PLS model (classification of degraded based on statistical comparison with reference group, for a p-value<0.02)

Table 3 – Comparison of PLS model prediction using ultrasonic spectra data for validation group

Sample	Sintering – surface voids area coverage				Degradation – zero-shear viscosity			
	Predicted value (%)	Observed value (%)	p-value	Incomplete sintering? (p<0.02)	Predicted value (Pa-s)	Observed value (Pa-s)	p-value	Degraded? (p<0.02)
201	5.4	3.9	<0.0001	Yes	6843	6447	0.36	No
214	2.6	3.2	0.006	Yes	8228	6541	0.001	Yes
220	3.1	2.6	0.006	Yes	10011	7622	0.0008	Yes
233	1.1	0.8	0.69	No	11187	12019	0.0001	Yes

4. Conclusions

A new nondestructive evaluation method was demonstrated to simultaneously evaluate both sintering and degradation phenomena in polyethylene rotational molded samples. Spectral amplitude at excitation frequencies can be used to evaluate the degree of sintering, with increase amplitude showing a reduction in attenuation caused by void concentration. This is a standard density evaluation. However, at the same time the amplitude of higher harmonics in the ultrasonic spectrum increased with increasing degradation. When compared to more traditional degradation characterization methods, the harmonic amplitude showed good correlation with the rheological data and higher sensitivity than FT-IR. A key point in favor of this new method for monitoring degradation is that greater damage has been shown to occur to the internal surfaces of the rotomolded parts, which are not accessible to nondestructive testing using FT-IR. PLS models showed their potential to estimate the values from the traditional methods and classify samples based on sintering and degradation properties, decoupling this spectroscopic approach from its earlier reliance on mechanical deformation to train the method to identify structural changes. Overall, this study demonstrates a new characterization method for rotational molded parts that not only can provide an alternative to current destructive techniques but also combines the observation of two distinctive phenomena in one single technique. The development of this method can represent a valuable additional tool for polymer processing industry to tackle the challenge towards advanced manufacturing, improving on process reliability and flexibility.

Acknowledgments

Special thanks to Ron Cooke at Imperial Oil Ltd (Sarnia, Ontario) for the technical support and materials provided to this project. Funding of this project was supported by Imperial Oil Ltd and Conselho Nacional de Desenvolvimento Científico e Tecnológico (CNPq) - Brazil through the Science Without Borders Scholarship Program.

References

- [1] B. Esmailian, S. Behdad, B. Wang, The evolution and future of manufacturing: A review, *J. Manuf. Syst.* 39 (2016) 79–100. doi:10.1016/j.jmsy.2016.03.001.
- [2] W.-C. Chen, P.-H. Tai, M.-W. Wang, W.-J. Deng, C.-T. Chen, A neural network-based approach for dynamic quality prediction in a plastic injection molding process, *Expert Syst. Appl.* 35 (2008) 843–849. doi:10.1016/j.eswa.2007.07.037.
- [3] Z. Jiang, Y. Yang, S. Mo, K. Yao, F. Gao, Polymer Extrusion: From Control System Design to Product Quality, *Ind. Eng. Chem. Res.* 51 (2012) 14759–14770. doi:10.1021/ie301036c.
- [4] K. Mitra, Genetic algorithms in polymeric material production, design, processing and other applications: a review, *Int. Mater. Rev.* 53 (2008) 275–297. doi:10.1179/174328008X348174.
- [5] D.I. Abu-Al-Nadi, D.I. Abu-Fara, I. Rawabdeh, R.J. Crawford, Control of rotational molding using adaptive fuzzy systems, *Adv. Polym. Technol.* 24 (2005) 266–277. doi:10.1002/adv.20047.
- [6] I. Gibson, D. Shi, Material properties and fabrication parameters in selective laser sintering process, *Rapid Prototyp. J.* 3 (1997) 129–136. doi:10.1108/13552549710191836.
- [7] M.J. Oliveira, M.C. Cramez, R.J. Crawford, Structure-properties relationships in rotationally moulded polyethylene, *J. Mater. Sci.* 31 (1996) 2227–2240. doi:10.1007/BF01152932.
- [8] M. Kontopoulou, J. Vlachopoulos, Bubble dissolution in molten polymers and its role in rotational molding, *Polym. Eng. Sci.* 39 (1999) 1189–1198. doi:10.1002/pen.11505.
- [9] A.G. Spence, R.J. Crawford, The effect of processing variables on the formation and removal of bubbles in rotationally molded products, *Polym. Eng. Sci.* 36 (1996) 993–1009. doi:10.1002/pen.10487.
- [10] E. Epacher, Processing stability of high density polyethylene: effect of adsorbed and dissolved oxygen, *Polymer (Guildf)*. 41 (2000) 8401–8408. doi:10.1016/S0032-3861(00)00191-9.
- [11] M.. Cramez, M.. Oliveira, R.. Crawford, Optimisation of rotational moulding of polyethylene by predicting antioxidant consumption, *Polym. Degrad. Stab.* 75 (2002) 321–327. doi:10.1016/S0141-3910(01)00234-8.

- [12] B.I. Chaudhary, E. Takács, J. Vlachopoulos, Processing enhancers for rotational molding of polyethylene, *Polym. Eng. Sci.* 41 (2001) 1731–1742. doi:10.1002/pen.10870.
- [13] A.C. Tavares, J. V. Gulmine, C.M. Lepienski, L. Akcelrud, The effect of accelerated aging on the surface mechanical properties of polyethylene, *Polym. Degrad. Stab.* 81 (2003) 367–373. doi:10.1016/S0141-3910(03)00108-3.
- [14] A. Saifullah, B. Thomas, R. Cripps, K. Tabeshfar, L. Wang, C. Muryn, Fracture toughness of rotationally molded polyethylene and polypropylene, *Polym. Eng. Sci.* 58 (2018) 63–73. doi:10.1002/pen.24531.
- [15] A.A. Mendes, A.M. Cunha, C.A. Bernardo, Study of the degradation mechanisms of polyethylene during reprocessing, *Polym. Degrad. Stab.* 96 (2011) 1125–1133. doi:10.1016/j.polymdegradstab.2011.02.015.
- [16] A.A. Cuadri, J.E. Martín-Alfonso, The effect of thermal and thermo-oxidative degradation conditions on rheological, chemical and thermal properties of HDPE, *Polym. Degrad. Stab.* 141 (2017) 11–18. doi:10.1016/j.polymdegradstab.2017.05.005.
- [17] J. V. Gulmine, P.R. Janissek, H.M. Heise, L. Akcelrud, Degradation profile of polyethylene after artificial accelerated weathering, *Polym. Degrad. Stab.* 79 (2003) 385–397. doi:10.1016/S0141-3910(02)00338-5.
- [18] M.C. Cramez, M.J. Oliveira, S. Fakirov, R.J. Crawford, A.A. Apostolov, M. Krumova, Rotationally molded polyethylene: Structural characterization by X-ray and microhardness measurements, *Adv. Polym. Technol.* 20 (2001) 116–124. doi:10.1002/adv.1009.
- [19] K. Adachi, Ultrasonic investigations of morphology and stress relaxation in drawn polypropylene, *22* (1981) 1026–1031.
- [20] A. Tanaka, K. Nitta, S. Onogi, Ultrasonic velocity and attenuation of polymeric solids under oscillatory deformation: apparatus and preliminary results, *Polym. Eng. Sci.* 29 (1989) 1124–1130.
- [21] A. Sahnoune, J. Tatibouët, R. Gendron, A. Hamel, L. PichÉ, Application of Ultrasonic Sensors in the Study of Physical Foaming Agents for Foam Extrusion, *J. Cell. Plast.* 37 (2001) 429–454. doi:10.1106/PEXL-PR2B-B1MH-47D3.
- [22] F.P.C. Gomes, M.R. Thompson, Analysis of Mullins effect in polyethylene using ultrasonic guided waves, *Polym. Test.* 60 (2017) 351–356. doi:10.1016/j.polymertesting.2017.04.020.
- [23] F.P.C. Gomes, W.T.J. West, M.R. Thompson, Effects of annealing and swelling to initial plastic deformation of polyethylene probed by nonlinear ultrasonic guided waves, *Polymer (Guildf)*. 131 (2017) 160–168. doi:10.1016/j.polymer.2017.10.041.
- [24] C.T. Bellehumeur, J.S. Tiang, Simulation of non-isothermal melt densification of polyethylene in rotational molding, *Polym. Eng. Sci.* 42 (2002) 215–229. doi:10.1002/pen.10942.

